Electronic Supplementary Material (ESI) for Journal of Materials Chemistry C.

Supporting Information for:

Pressure-induced structural phase transition, irreversible amorphization and upconversion luminescence enhancement in Ln^{3+} codoped $LiYF_4$ and $LiLuF_4$

Yingying Ma, [a] Ting Wen, *[a] Ke Liu, [a] Dequan Jiang, [b] Mei-Huan Zhao, [c] Chuanlong Lin, [a] and Yonggang Wang* [a,b]

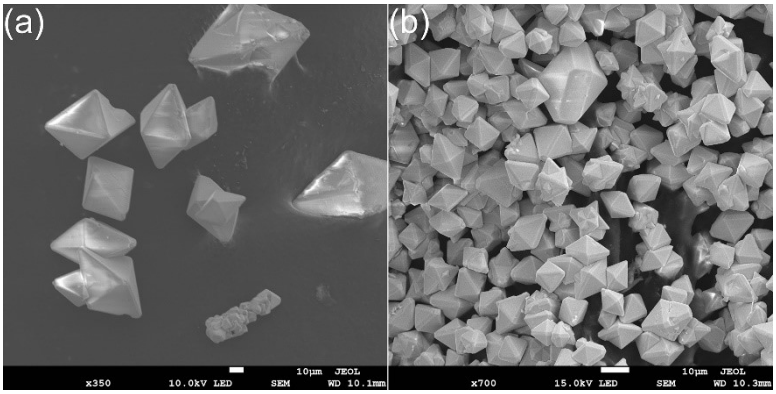

Fig. S1 SEM images of (a) $LiYF_4$ and (b) $LiLuF_4$.

Table 1. The calculated lattice parameters for undoped and Ln^{3+} doped $LiYF_4$ and $LiLuF_4$ samples.

Samples	Space group	a(Å)	c(Å)	V(Å^3)
$LiYF_4$	$I4_1/a$	5.1695(1)	10.7309(1)	286.77(1)
$LiYF_4$:19%Yb^{3+}/1%Er^{3+}		5.1679(1)	10.7225(3)	286.37(2)
$LiYF_4$:19%Yb^{3+}/1%Ho^{3+}		5.1675(1)	10.7194(3)	286.24(1)
$LiYF_4$:19.9%Yb^{3+}/0.1%Tm^{3+}		5.1672(1)	10.7196(3)	286.21(1)
$LiLuF_4$		5.1261(1)	10.5440(2)	277.06(1)
$LiLuF_4$:19%Yb^{3+}/1%Er^{3+}		5.1296(1)	10.5583(1)	277.82(1)
$LiLuF_4$:19%Yb^{3+}/1%Ho^{3+}		5.1293(1)	10.5576(1)	277.77(1)
$LiLuF_4$:19.9%Yb^{3+}/0.1%Tm^{3+}		5.1290(1)	10.5557(1)	277.69(1)

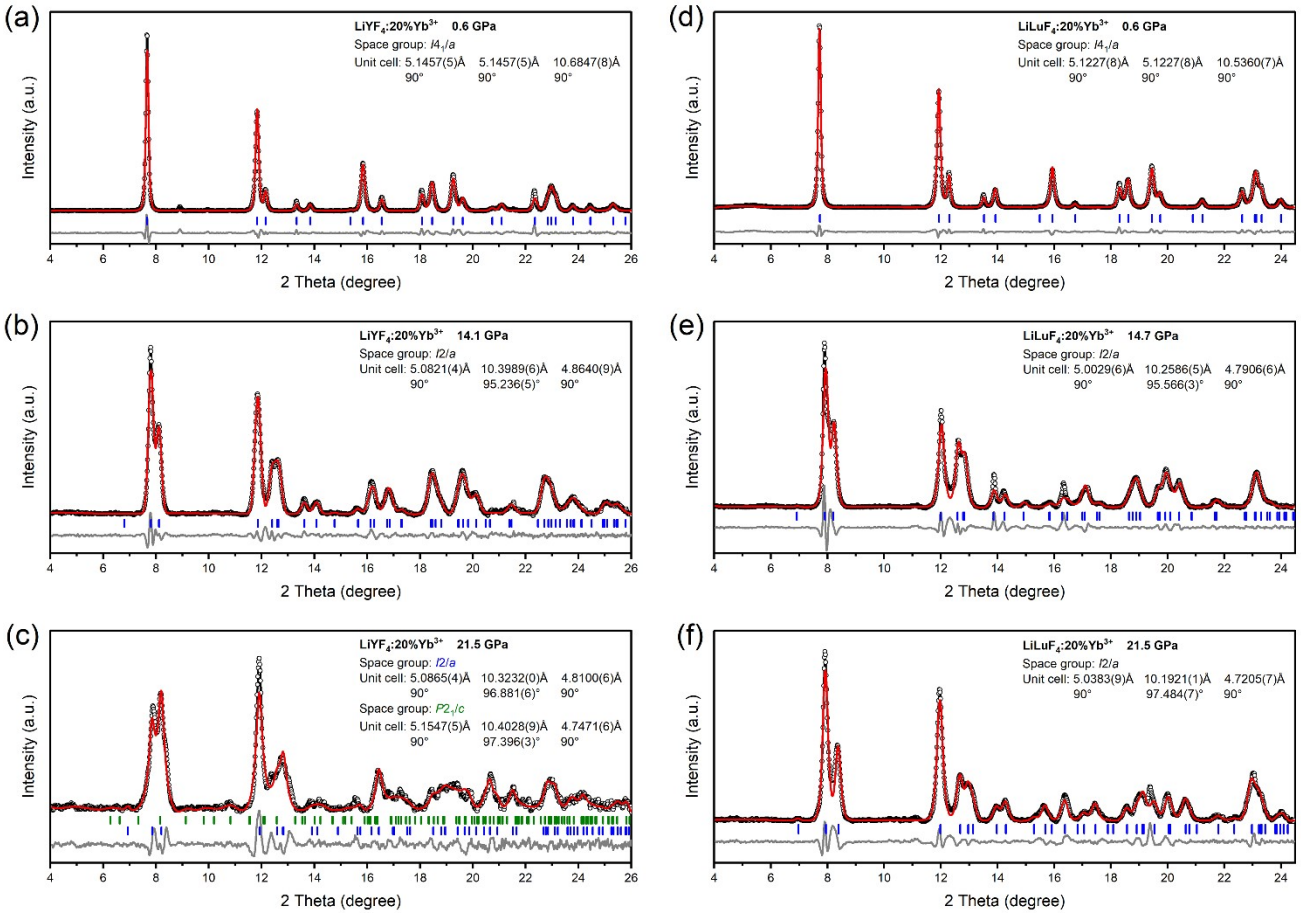

Fig. S2 Le Bail refinement based on the powder XRD data of (a) $LiYF_4$:20%Yb^{3+} at 0.6 GPa; (b) $LiYF_4$:20%Yb^{3+} at 14.1 GPa; (c) $LiYF_4$:20%Yb^{3+} at 21.5 GPa; (d) $LiLuF_4$:20%Yb^{3+} at 0.6 GPa; (e) $LiLuF_4$:20%Yb^{3+} at 14.7 GPa; (f) $LiLuF_4$:20%Yb^{3+} at 21.5 GPa.

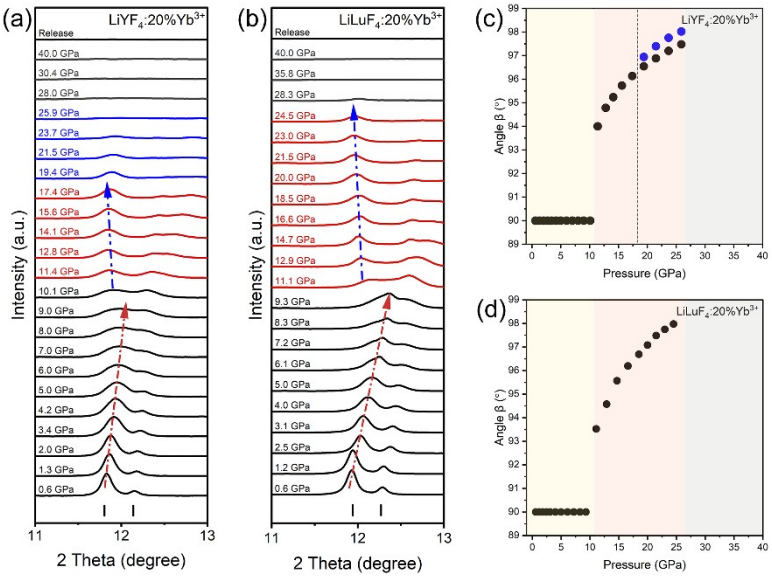

Fig. S3 Enlarged XRD patterns in the 2θ range of 11° to 13° in (a) $LiYF_4$:20%Yb^{3+} and (b) $LiLuF_4$:20%Yb^{3+}, respectively. Pressure dependence of angle β of (c) $LiYF_4$:20%Yb^{3+} and (d) $LiLuF_4$:20%Yb^{3+}, respectively.

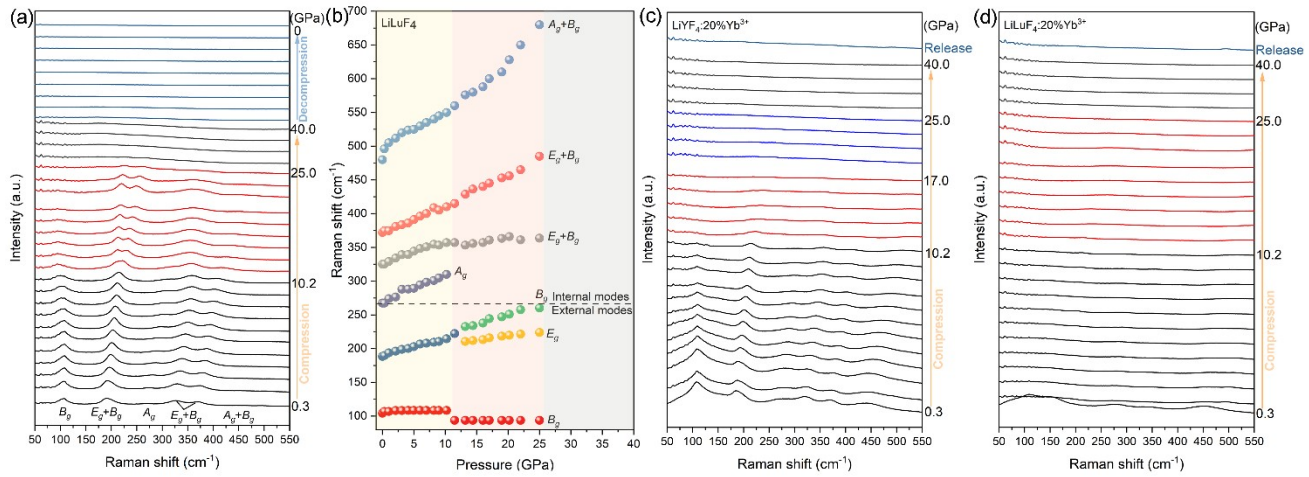

Fig. S4 Raman spectra of (a) $LiLuF_4$, (c) $LiYF_4$:20%Yb^{3+} and (d) $LiLuF_4$:20%Yb^{3+} under compression and decompression. (b) Pressure dependence of the Raman peak positions in the wavenumber range of 50~600 cm^{-1} in $LiLuF_4$.

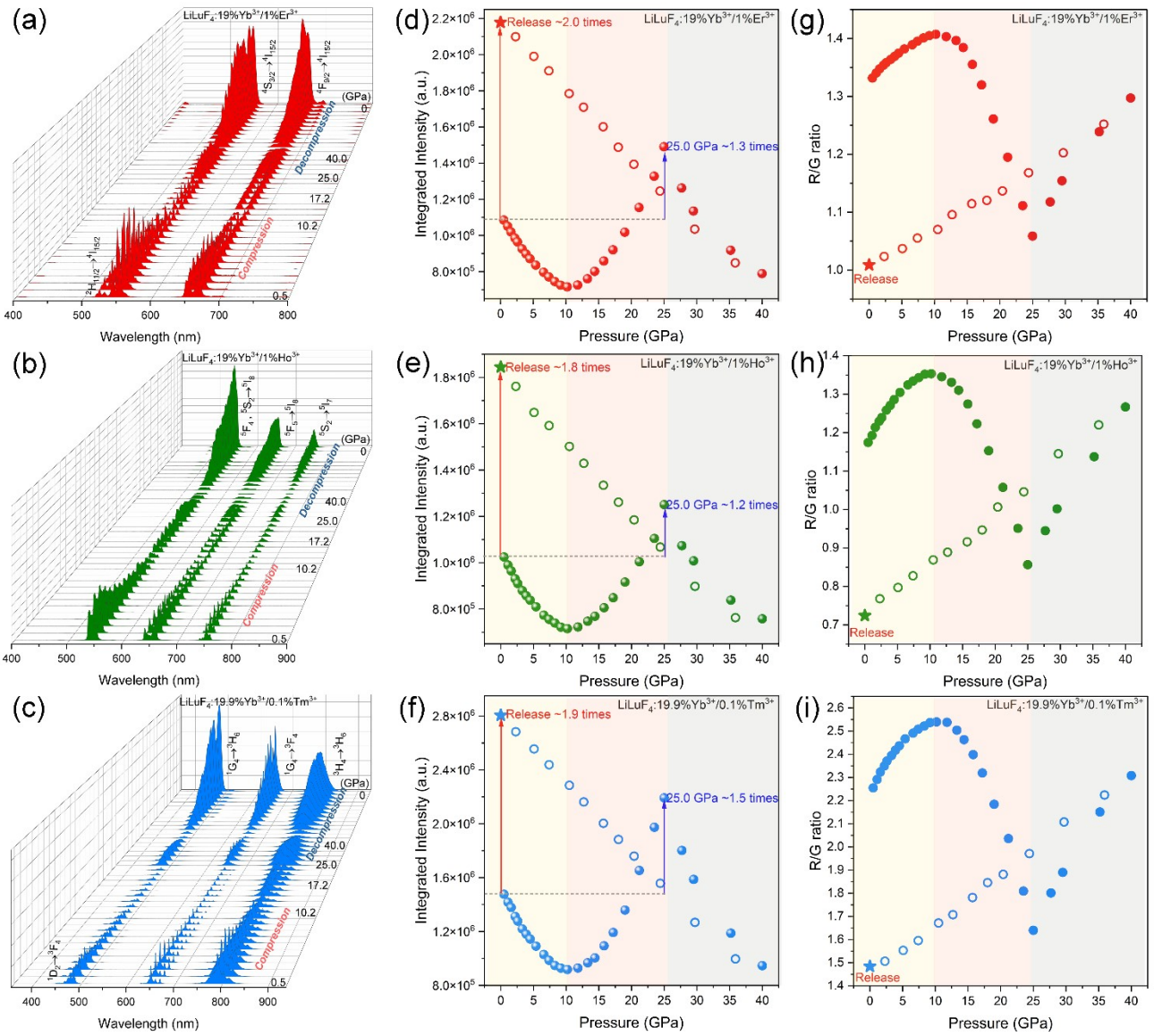

Fig. S5 UC PL spectra of (a) $^2H_{11/2}\rightarrow{}^4I_{15/2}$, $^4S_{3/2}\rightarrow{}^4I_{15/2}$ and $^4F_{9/2}\rightarrow{}^4I_{15/2}$ in LiLuF$_4$:19%Yb^{3+}/1%Er^{3+} (b) $^5F_4$,$^5S_2\rightarrow{}^5I_8$, $^5F_5\rightarrow{}^5I_8$ and $^5S_2\rightarrow{}^5I_7$ in LiLuF$_4$:19%Yb^{3+}/1%Ho^{3+} (c) $^1D_2\rightarrow{}^3F_4$, $^1G_4\rightarrow{}^3H_6$, $^1G_4\rightarrow{}^3F_4$, and $^3H_4\rightarrow{}^3H_6$ in LiLuF$_4$:19.9%Yb^{3+}/0.1%Tm^{3+} under compression and release cycle. (d), (e), (f) Pressure-dependent UC luminescence total intensity evolution. The relative intensity ratios (R/G) of (g) red ($^4F_{9/2}\rightarrow{}^4I_{15/2}$) and green ($^2H_{11/2}\rightarrow{}^4I_{15/2}$, $^4S_{3/2}\rightarrow{}^4I_{15/2}$), (h) red ($^5F_5\rightarrow{}^5I_8$, $^5S_2\rightarrow{}^5I_7$) and green ($^5F_4$,$^5S_2\rightarrow{}^5I_8$) and (i) red ($^1G_4\rightarrow{}^3F_4$, $^3H_4\rightarrow{}^3H_6$) and green ($^1D_2\rightarrow{}^3F_4$, $^1G_4\rightarrow{}^3H_6$) band transition of *Ln*$^{3+}$ codoped LiLuF$_4$ under pressure.

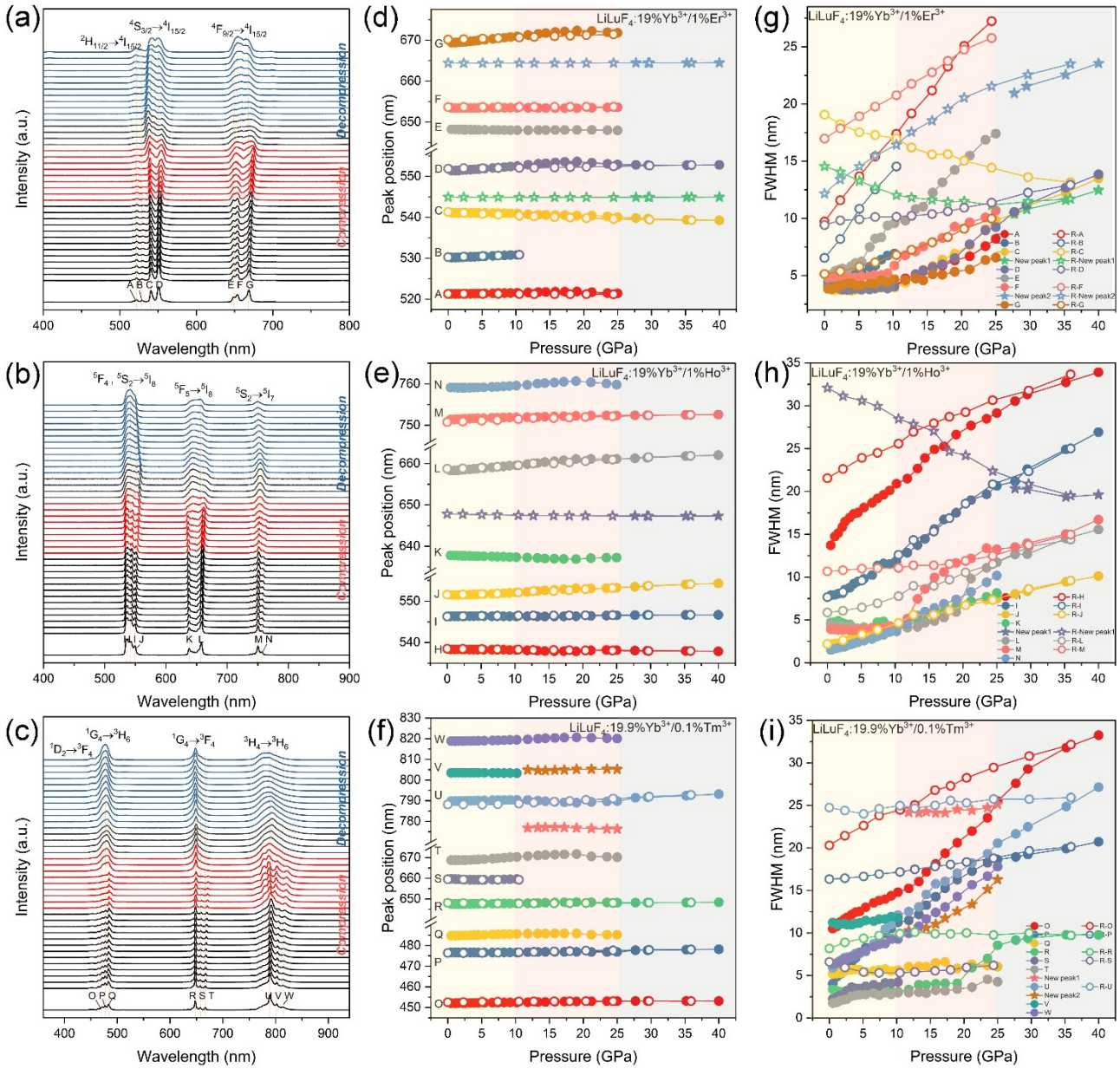

Fig. S6 Resolved sublevels of (a) $LiLuF_4$:19%Yb^{3+}/1%Er^{3+} (b) $LiLuF_4$:19%Yb^{3+}/1%Ho^{3+} (c) $LiLuF_4$:19.9%Yb^{3+}/0.1%Tm^{3+} under compression and decompresssion. (d), (e), (f) Pressure dependence of peak position of individually resolved sublevels. (g), (h), (i) The FWHM of individually resolved sublevels as a function of pressure.

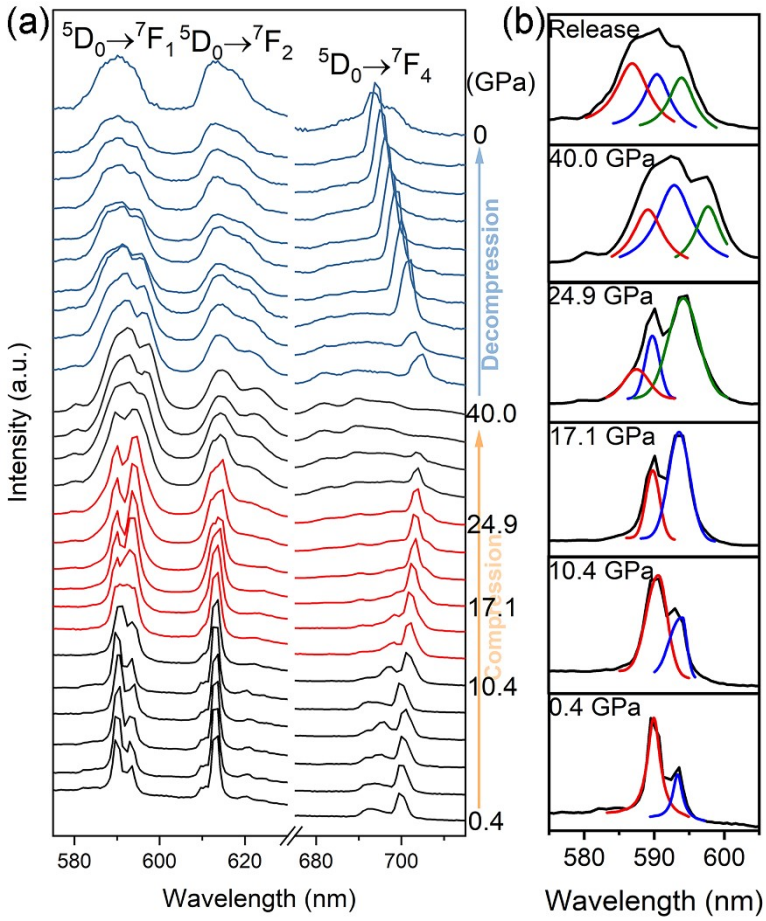

Fig. S7 (a) Emission spectra of $LiLuF_4$:19%Yb^{3+}/1%Eu^{3+} under compression and decompression. (b) multipeak fitting of $^5D_0 \rightarrow {}^7F_1$ at selected pressures.